Hydrous bioethanol production from sugarcane bagasse via energy self-sufficient gasification-fermentation hybrid route
Simulation and financial analysis

de Medeiros, Elisa M.; Posada, John A.; Noorman, Henk; Osseweijer, Patricia; Filho, Rubens Maciel

DOI
10.1016/j.jclepro.2017.01.165

Publication date
2017

Document Version
Final published version

Published in
Journal of Cleaner Production

Citation (APA)
de Medeiros, E. M., Posada, J. A., Noorman, H., Osseweijer, P., & Filho, R. M. (2017). Hydrous bioethanol production from sugarcane bagasse via energy self-sufficient gasification-fermentation hybrid route: Simulation and financial analysis. *Journal of Cleaner Production*, *168*, 1625-1635. https://doi.org/10.1016/j.jclepro.2017.01.165

Journal of Cleaner Production 168 (2017) 1625–1635

Contents lists available at ScienceDirect

Journal of Cleaner Production

journal homepage: www.elsevier.com/locate/jclepro

Hydrous bioethanol production from sugarcane bagasse via energy self-sufficient gasification-fermentation hybrid route: Simulation and financial analysis

Elisa M. de Medeiros [a, b, *], John A. Posada [b], Henk Noorman [b, c], Patricia Osseweijer [b], Rubens Maciel Filho [a]

[a] Faculdade de Engenharia Química, University of Campinas (UNICAMP), Av. Albert Einstein 500, 13084-852, Campinas, SP, Brazil
[b] Department of Biotechnology, Delft University of Technology, van der Maasweg 9, 2629 HZ, Delft, The Netherlands
[c] DSM Biotechnology Center, PO Box 1, 2600 MA, Delft, The Netherlands

ARTICLE INFO

Article history:
Received 16 August 2016
Received in revised form
24 January 2017
Accepted 30 January 2017
Available online 1 February 2017

Keywords:
Second generation bioethanol
Biomass gasification
Syngas fermentation
Process simulation
Aspen plus
Financial analysis

ABSTRACT

Production of second generation ethanol can be accomplished with biomass gasification followed by syngas fermentation using acetogenic bacteria in a hybrid process. Using process simulation and financial analysis, this study evaluated the feasibility of producing hydrous ethanol from sugarcane bagasse in a conceptual hybrid plant designed to be energetically self-sufficient. The process was found to be competitive with other second generation routes, achieving an ethanol yield of 330 L per metric ton of dry biomass and an overall carbon conversion of 30%. The minimum ethanol selling price to achieve Net Present Value break-even with 10% Internal Rate of Return was estimated to be 706 US$/m^3 after taxes in the base model. When accounting for uncertainties in the fixed capital investment and the cost of raw materials, the Net Present Value was found to be non-negative in 80% of the cases for a selling price of 783 US$/m^3.

1. Introduction

Hydrous bioethanol (E100), a solution of ethanol and water near the azeotrope composition (93–95 wt% ethanol), is largely used in Brazil as a biofuel in flexible-fuel light vehicles. Due to its cost competitiveness with gasoline and growing public concern over issues of environmental and energy security, E100 production and sales have increased at fast rates, a trend which is expected to continue. In 2015, for example, E100 consumption saw a 37.5% increase compared to the previous year, accounting for more than 17.8 billion litres consumed nationwide (UNICA, 2016). In Brazil, the widespread commercialization of E100 reflects the well-established industry built on mature 1st-generation technology for sugarcane production, extraction, fermentation and ethanol distillation. However, while the use of bioethanol as substitute (or additive) for gasoline may effectively reduce the emissions of fossil-originated carbon dioxide, the massive expansion of sugarcane and other crops may result in significant environmental impacts, such as soil degradation, contamination of aquatic systems and eutrophication due to use of fertilizers and herbicides, and emissions of nitrous oxide (a strong greenhouse gas), also associated to the use of fertilizers (Souza et al., 2015). In this context, efforts to minimize environmental damage and increase sustainability indices in biofuels and biobased products sectors have boosted scientific research on 2nd-generation technology, *i.e.* the conversion of lignocellulosic biomass (Cheali et al., 2015) or wastes (Fernández-

Abbreviations: CAPEX, capital expenditure; C_{OL}, cost of operating labor; C_{RM}, cost of raw materials; C_{UT}, cost of utilities; C_{WT}, cost of waste treatment/disposal; CW, cooling water; CZ, combustion zone; d, depreciation; DPC, direct production cost; E100, hydrous ethanol fuel; FC, fixed carbon; FCI_L, fixed capital investment excluding land purchase cost; FPC, fixed production cost; GE, general expenses; GZ, gasification zone; GRT, gas retention time; HHV, higher heating value; IRR, Internal Rate of Return; LRT, liquid retention time; MCS, Monte Carlo simulation; MED, multiple-effect distillation; MESP, minimum ethanol selling price; NPV, Net Present Value; NRTL, non-random two-liquid model; NRTL-HOC, non-random two-liquid model with Hayden O'Connell equation-of-state; OPEX, operating expenditures; PCE, purchase cost of equipment; PFD, process flow diagram; Q_c, cooling requirement in distillation condenser; Q_r, heating requirement in distillation reboiler; RKS-EOS, Redlich-Kwong-Soave equation-of-state; STBR, steam to biomass ratio; VM, volatile material; WGS, water-gas shift reaction.

* Corresponding author. Faculdade de Engenharia Química, University of Campinas (UNICAMP), Av. Albert Einstein 500, 13084-852, Campinas, SP, Brazil.
E-mail address: elisamedeiros@feq.unicamp.br (E.M. de Medeiros).

http://dx.doi.org/10.1016/j.jclepro.2017.01.165
0959-6526/

Dacosta et al., 2015) to biofuels and biochemicals.

Traditionally, two main platforms are considered for the conversion of lignocellulose to ethanol, namely: *i*) a biochemical platform comprising biomass pre-treatment, hydrolysis and sugars fermentation; and *ii*) a thermochemical platform comprising biomass gasification and syngas conversion to ethanol. The latter conversion can be accomplished via two distinct pathways: a high-pressure, metal-based catalytic conversion, which characterizes a thermochemical-catalytic process (usually called simply the thermochemical route); and a biological conversion (*i.e.* fermentation), characterizing a thermochemical-biochemical (hybrid) process. Although less popular than the other pathways, the so-called hybrid pathway has received growing attention in the past years, both inside and outside academic circles. For example, Lanzatech, one of the companies seeking to commercialize the fermentation of syngas or waste gas from steel production, has been attracting special media attention (Lane, 2015).

Ethanol can be produced by strictly anaerobic, mostly mesophilic, bacteria that are capable of autotrophically converting CO, CO_2 and H_2 according to Eqs. (1) and (2) as result of the Wood-Ljungdahl metabolic pathway (Vega et al., 1989). This process has been reported to offer several advantages over catalytic conversion, such as higher yields, higher reaction specificity, lower energy requirements, syngas composition flexibility and higher resistance to contaminants (Klasson et al., 1992). Furthermore, gasification of biomass is feedstock-flexible and capable of utilizing all biomass components, including lignin, while dismissing complex pre-treatment and avoiding the use of expensive enzyme cocktails (Shen et al., 2015). Notwithstanding these potential advantages, syngas fermentation is still at an early stage of technological development compared to other conversion routes and therefore requires improvements and better understanding of several processing aspects. For example, there are several open issues regarding unsettled parameters, such as: *(i)* threshold resistance of microorganisms to syngas contaminants; *(ii)* optimal conditions and bioreactor design for ethanol production; and *(iii)* optimal integration between gasification, syngas fermentation and distillation; among others.

$$6CO + 3H_2O \rightarrow C_2H_5OH + 4CO_2 \quad (1)$$

$$2CO_2 + 6H_2 \rightarrow C_2H_5OH + 3H_2O \quad (2)$$

Despite the increasing number of publications regarding syngas fermentation, only a few articles have presented techno-economic or environmental assessments of integrated processes based on this technology. Piccolo and Bezzo (2009) performed process design, heat integration and economic assessment to evaluate the feasibility of a hybrid route in comparison with enzymatic hydrolysis followed by fermentation, finding the latter to be more financially attractive. Wei et al. (2009), using a black-box system model based on literature data, concluded that, from a process engineering perspective, the hybrid gasification-fermentation route would be less feasible than both hydrolysis followed by sugars fermentation and gasification followed by chemical synthesis. Moreover, an optimization study delivered by Martín and Grossmann (2011) regarding technological routes for lignocellulosic ethanol production via gasification demonstrated chemical synthesis to be a better choice for syngas conversion than syngas fermentation, although the authors also reported promising results of production costs. In contrast, Wagner and Kaltschmitt (2012), using process simulation in Aspen Plus to compare the three types of pathway, found gasification followed by syngas fermentation to be the most energy efficient process. More recently, Roy et al. (2015) evaluated the production cost and greenhouse gas emissions for four scenarios using the hybrid route for ethanol production and arrived at promising results, especially if untreated feedstock is used. Besides these examples, the production of other products through syngas fermentation has also been assessed by Choi et al. (2010), who demonstrated the viability of producing polyhydroxyalkanoate (PHA) and H_2 through this route.

In this study, a process design has been proposed for the production of hydrous ethanol (E100) from sugarcane bagasse using gasification and syngas fermentation in an energy self-sufficient plant. For this purpose, literature data and engineering skills have been combined in the development of a predictive model for further assessments. Unsettled issues, *e.g.* concerning effects of syngas contaminants on biological productivity, have been simplified but are explicitly addressed in the text. Important issues such as water consumption, carbon conversion, energy production and efficient concentration of highly dilute ethanol were addressed. A complete and integrated process flowsheet – from biomass residues to syngas, and from syngas to E100 and power –was designed and simulated in Aspen Plus using Hierarchy blocks to separate the different units in the process. Furthermore, a financial model was built to estimate the capital expenditure (*CAPEX*) and the operating expenditures (*OPEX)*, and to probabilistically estimate the minimum ethanol selling price (*MESP*) via Monte Carlo simulation.

2. Methodology

The approach is based on quantitative results generated by professional process simulators using up-to-date literature information on biomass gasification and syngas fermentation with acetogenic bacteria. The separation flowsheet adopts rigorously modeled multiple-effect distillation to cut heat consumption.

2.1. Process design and simulation

The commercial software Aspen Plus was used to simulate the conceptual integrated process for E100 production from sugarcane bagasse via the hybrid route: biomass gasification and syngas fermentation. The plant capacity is assumed to be 624 dry metric tons of bagasse per day, which is a compatible figure considering a medium scale sugarcane processing plant of roughly 1.7 million metric tons of sugarcane per harvest.

Material and energy balances were calculated for the proposed process flow diagram (PFD) in Aspen Plus environment from user-specified inlet streams, unit operations and additional subroutines. Aspen PFDs are available in Appendix A in the Supplementary Material. A simplified block flow diagram of the process is depicted in Fig. 1, with the respective Aspen PFD in Fig. A-1 (Appendix A, Supp. Material). The following sections (2.1.1 to 2.1.5) provide specific details on the simulation methodology applied for each unit. When relevant, block models and stream/block names are parenthesized to facilitate their identification in the Aspen PFDs. It is recommended that the reader follows the text with the flowsheets at hand for easier comprehension.

2.1.1. Gasification unit (A100)

The Gasification Unit (Fig. A-2, Supp. Material) comprises the following unit operations: biomass feed handling and drying; indirectly-heated gasification in dual circulating fluidized bed; and cyclone removal of particulates. This type of gasifier consists of two separate, interconnected, beds, through which hot bed material circulates and transfers heat between different zones. In the gasification zone (GZ) bed, steam is added as sole gasifying agent, while in the combustion zone (CZ) bed, air is added as combustion agent. With this configuration, high quality syngas, with higher concentration of H_2 and no dilution in N_2, can be produced. The simulation

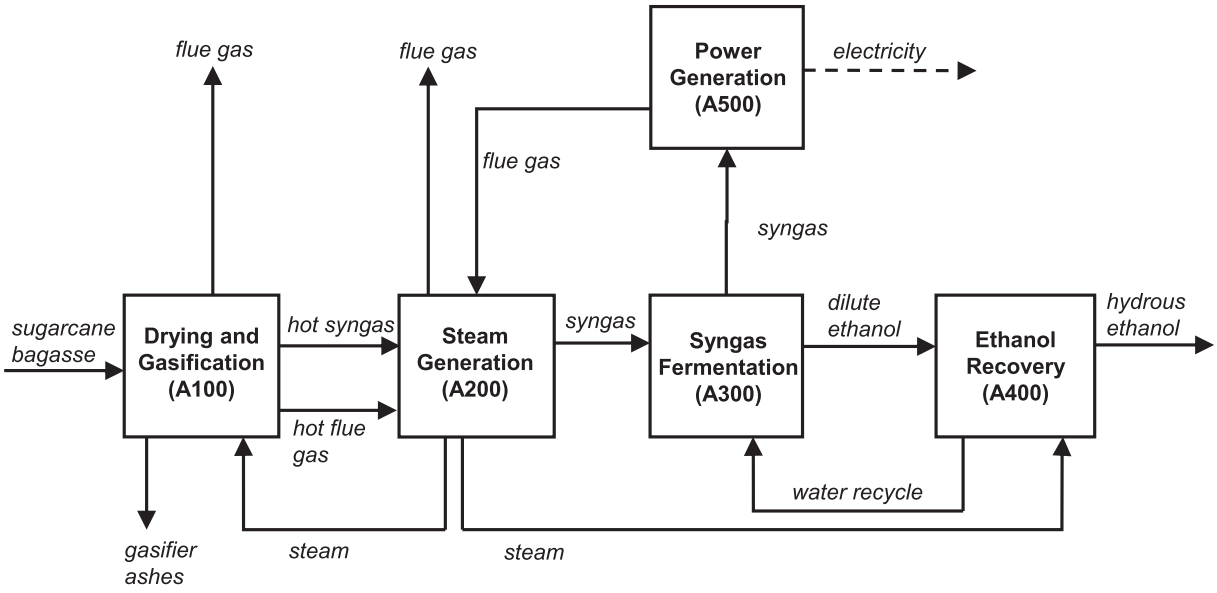

Fig. 1. Simplified block flow Diagram of E100 production from sugarcane bagasse via gasification and syngas fermentation.

assumes no energy losses and achievement of equilibrium conditions, and thermodynamic properties are calculated using the Redlich-Kwong-Soave equation of state (RKS-EOS).

In this unit, wet sugarcane bagasse (stream LCM-IN) is fed with a mass flow rate of 52,000 kg/h and a moisture content of 50 wt%, which is then reduced to 10 wt% in a rotary dryer using hot flue gases from the combustion of a fraction of the char that is formed during the pyrolysis reactions that take place in the gasifier. The RYield block RD simulates drying of moisture with hot gases, while the cyclone separator RD-CYC separates gas and solid phases after drying. Biomass is modeled in Aspen Plus as a non-conventional component characterized by the component attributes specified in Table 1. Proximate and ultimate analyses were obtained from the simulation of a sugarcane processing plant as described by Bonomi et al. (2011). The higher heating value (HHV) was calculated using the correlation formulated by Parikh et al. (2005). Since non-conventional components do not participate in phase and chemical equilibrium calculations, an RYield reactor model (block DCMP) is firstly used to decompose biomass into its constituent elements (C, H_2, O_2, N_2, Cl, S, H_2O) to enable the subsequent calculations. Although this stage of decomposition (not to be confused with pyrolysis) is not observed in reality, it configures an effective resource to quantitatively simulate operations with heterogeneous solids (Aspen Technology, 2011) such as biomass gasification (Ramzan et al., 2011), and its enthalpy change must be accounted for in the heat balance.

The gasifier itself consists of two fluidized beds with circulation of bed material (olivine) which is responsible for heat transfer between the CZ and the GZ. Pre-heated air at 130 °C is fed into the CZ (RStoic model), where char is burned to provide heat for the endothermic gasification reactions. The separator S-1 represents the separation of the char fraction that is used for combustion. The GZ (RGibbs model) is fed with biomass and saturated steam (STM-GSF) which acts as gasifying agent at 2.5 bar (127.5 °C). The steam-to-biomass ratio (STBR), defined here as the mass ratio of steam plus biomass moisture to dry biomass, is 0.34, a value which was chosen inside the typical range of 0.2–2, with a preference for lower values due to lower energy consumption (Silva and Rouboa, 2014). The temperatures in the GZ and the CZ are assumed to be 950 °C and 1000 °C, respectively, which is consistent with operating ranges reported for this type of gasifier (Brown, 2011; Worley and Yale, 2012). The gas then passes through a cyclone (CYC) to remove particulates. Although the simulation neglects tar formation, the economic evaluation assumes that the gasifier module represents both a gasifier and a tar reformer which catalytically converts hydrocarbons into CO and H_2, thereby approaching equilibrium conditions. As a matter of fact, it is a reasonable approximation to assume equilibrium composition at the tar reformer outlet since the catalyst shows significant water-gas-shift (WGS) activity (Dutta et al., 2011).

Syngas compositions and yields are strongly affected by a number of parameters, such as biomass composition and size, gasifier temperature and STBR (Puig-Arnavat et al., 2010). In order to avoid modeling unnecessary complex kinetics related to the large number of reactions taking place during gasification and reforming in this preliminary conceptual design, the gasifier model adopts a multi-reaction equilibrium approach with considerations of operating conditions that would in fact favor the achievement of equilibrium (*i.e.* very high temperature and use of tar reforming catalysts). This is a common approach for gasifier models reported in the literature (Baratieri et al., 2008; Esmaili et al., 2016; Van der Heijden and Ptasinski, 2012). Although complete equilibrium conditions are unlikely in real operations, equilibrium models are very important to the design of chemical processes, as they set limiting

Table 1
Sugarcane bagasse component attributes.

Ultimate Analysis (wt%, daf)						Proximate Analysis (wt%, db)				HHV (db) ($MJ.kg^{-1}$)
C	H	O	N	Cl	S	FC	VM	Ash	Moisture	
46.96	5.72	44.05	0.27	0.02	0.04	18.00	79.06	2.94	50.00	18.5

daf: dry-ash-free basis; db: dry basis; FC: fixed carbon; VM: volatile material.

operation performances. As a notable example, distillation columns and sour gas absorbers with aqueous ethanolamines are commonly sized using equilibrium approach models, but rarely operate at strict equilibrium conditions. In the same way, it is evident that the equilibrium approach simplifies the gasifier model, but it does not undermine significantly the integrated process, given the high temperature conditions which accelerate kinetics driving the real reactor performance to near equilibrium. Taking into account that the final goal of this work is an overall assessment that considers several concomitant sources of uncertainty within a Monte Carlo framework, it is reasonable to consider that the relaxation brought by modeling the gasification step with multi-reaction chemical equilibrium is not sufficient to compromise the final results and/or our conclusions.

2.1.2. Steam generation unit (A200)

The heat exchanger network in A200 (Fig. A-3, Supp. Material) consists of five heat exchangers (E-1 to E-5) producing process steam by cooling of hot gases. Two categories of steam are produced in this unit: *(i)* 2.5 bar saturated steam, used as utility and gasifying agent; and *(ii)* 10 bar saturated steam, used as utility. The hot inlet gases are: *(i)* syngas from A100 (H-SYNGAS); *(ii)* hot flue gas from the CZ in A100 (H-GAS-1); and *(iii)* hot exhaust from the gas turbine in A500 (H-GAS-3). The liquid streams W2B-1 and W10B-1 are the steam utilities return as saturated liquid, while WGSF-1 is a fresh water stream directed for the production of steam for the gasification unit.

Heat from syngas is recovered until it reaches a temperature of 73 °C. The cooling water (CW) then continues with heat removal until 60 °C, which is assumed to be the syngas inlet temperature at the Venturi scrubber (VS). The scrubbing water (W-VS) is specified with a flow rate to provide a liquid to gas volumetric ratio (L/G) of 1 L/m^3, according to Dutta et al. (2011). The W-VS is maintained inside a closed loop with makeup and purge of approximately 8% of the recirculating flow rate. The liquid purge (WW-1) is sent to off-site wastewater treatment. The cold syngas, leaving the scrubber at a temperature of 54 °C, is sent to fermentation in A300.

2.1.3. Syngas fermentation unit (A300)

A300 (Fig. A-4, Supp. Material) consists essentially of a bioreactor, a microfiltration system for cell separation and a CO_2 scrubber for recovery of ethanol vapors from the fermenter off-gas. In this unit, A300, the property method NRTL-HOC was used due to the highly non-ideal mixture containing ethanol, water and acetic acid, which dimerizes in the vapor phase. Henry's Law was used as ideality model for reference state calculations of the light gases CO, CO_2 and H_2 in the aqueous phase.

Several types of bioreactor have been reported for syngas fermentation with different operating modes (continuous, batch or semibatch), for example: stirred tank (Klasson et al., 1991), bubble column (Rajagopalan et al., 2002), trickle bed (Klasson et al., 1991), hollow fiber membrane (Shen et al., 2014a) and monolithic biofilm reactors (Shen et al., 2014b). The process herein represented is based on a model that considers the experimental data reported by Gaddy et al. (2007) for syngas fermentation in a continuous agitated tank with water and cell recycle. Vapor-Liquid Equilibrium between the contacting phases in the fermenter is described by two blocks: *(i)* a stoichiometric reactor (FM) which simulates the fermentation reactions; and *(ii)* a flash separator (S-1) which properly separates the off-gas (OGAS-1) and the liquid phase broth (BRTH-1). The bioreactor is kept at 37 °C by chilled water entering at 15 °C and leaving at 25 °C. Two heat exchangers (E-1 and E-2) are used to cool the reactor liquid inlet which is composed mostly of recycle water from distillation.

Experimental results of continuous and steady state syngas fermentation using the strain *Clostridium ljungdahlii* with water and cell recycle were retrieved from the US Patent 7,285,402 B2, Example 15 (Gaddy et al., 2007). Although other authors have reported low ratios of ethanol to acetate in the broth (Richter et al., 2013; Younesi et al., 2005), Gaddy et al. (2007) reported high productivities of ethanol with nearly zero acetate production when using water and cell recycle. According to the authors, recycling the water from distillation which contains small amounts of acetate is an effective measure to enhance ethanol production, as acetate inhibition is promoted after it reaches concentration levels between 3 g/L and 5 g/L, hence leading to zero net acetate production and more carbon conversion to ethanol.

In order to simplify the model and enable its construction in Aspen environment, the following assumptions are considered: *(i)* by recycling aqueous broth with dilute acetic acid after distillation, there is no net acetic acid production due to the establishment of equilibrium between ethanol and acetic acid, hence acetic acid concentration in the reactor remains constant and the only reactions occurring are represented by Eqs. (1) and (2); *(ii)* concentration of cells remains approximately constant at 3 g/L with 100% cell recycle after separation by microfiltration (MF), therefore it is assumed that carbon consumed for cell production and maintenance is negligible; *(iii)* conversions of 90% of CO and 60% of H_2 are achieved; *(iv)* Liquid Retention Time (*LRT*) ≈ 23 h (volume of liquid in the reactor divided by liquid volumetric flow rate); and *(v)* Gas Retention Time (*GRT*) ≈ 12 min (volume of liquid in the reactor divided by inlet gas volumetric flow rate).

Applying these assumptions, broth concentrations around 23 g/L of ethanol, 6 g/L of acetic acid and 3 g/L of cells should be achieved (Gaddy et al., 2007). The total volume required for fermentation is directly obtained from the choice of GRT and the syngas flow rate, which is a known result from the upstream flowsheet. The assumption of negligible biomass production is supported by the fact that ethanol formation is usually not associated with growth in the Wood/Ljungdahl pathway (Richter et al., 2013). The CO_2 scrubber (block S) is modeled in Aspen as an absorption (RadFrac) column using sufficient water feed to recover roughly 95% of ethanol vapors. The scrubber gas outlet, containing unreacted CO and H_2, is sent to the gas turbine in the Power Generation Unit (A500).

2.1.4. Ethanol distillation unit (A400)

With approximately 2 wt% of ethanol, the broth obtained from syngas fermentation is highly diluted compared to the broth from sugars fermentation, leading to an even more energy intensive recovery by distillation. Nevertheless, given the state of the art of separation technologies, distillation remains as the best alternative at hand and this evaluation can serve as baseline for future investigations on other separation processes. The Aspen PFD of A400 is shown in Fig. A-5 (Supp. Material), while Fig. 2 illustrates the distillation configuration considered.

In order to reduce energy consumption, heat integration is proposed in a pre-concentration step (Fig. 2) where three similar towers, T-1, T-2 and T-3, operating at different pressures are used in an arrangement of multiple-effect distillation (MED) to concentrate ethanol up to about 15 wt%, after which it is sent to a fourth atmospheric column (T-4) where hydrous ethanol at 93 wt% is obtained as distillate.

Heat integration of distillation columns using multiple-effect technique seeks to reduce energy consumption by linking the condenser of a higher pressure column to the reboiler of a lower pressure column (Linnhoff et al., 1983). Many configurations of MED systems have been studied based on different combinations of number of effects, column pressures and feed-splitting, among other factors (Chiang and Luyben, 1983; Henley and Seader, 1981;

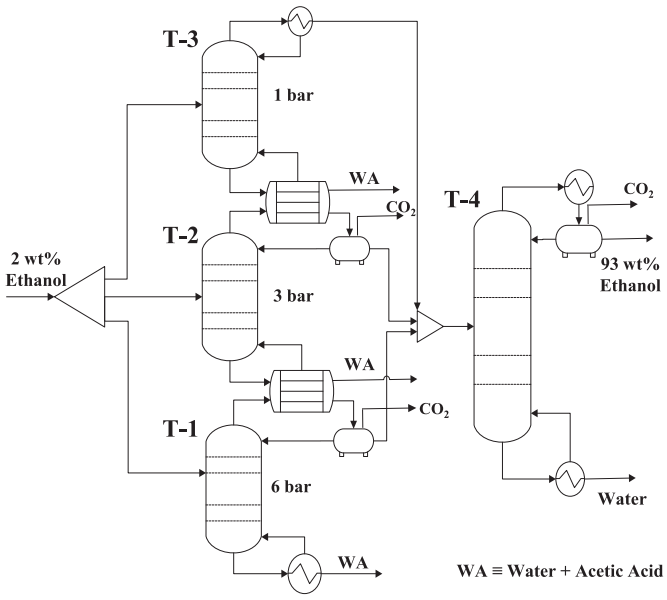

Fig. 2. Configuration of distillation columns for recovery of E100.

Wankat, 1993). As Chiang and Luyben (1983) remarked, such MED systems and other energy-saving configurations were seldom used in the past when energy costs were low, since savings would easily be offset by higher capital costs. However, in the past decades, the increase in energy costs at a much faster rate than equipment costs has drawn attention to energy-saving schemes such as MED, especially for application in large-scale processes. Recently, for example, Dias et al. (2011) and Palacios-Bereche et al. (2015) evaluated the use of double-effect distillation in the production process of 1st -generation ethanol from sugarcane, with one of the columns operating under vacuum. Similarly, Martín and Grossmann (2011), studying routes for the production of lignocellulosic ethanol, proposed a triple-effect distillation arrangement with the first two columns under vacuum.

In the present study, vacuum distillation columns were avoided due to higher costs and more complex control of cascaded vacuum systems, besides the need for larger column diameters. Therefore, the proposed MED scheme uses distillation columns operating at 6 bar, 3 bar and 1 bar, with respective reflux ratios of 0.20, 0.26 and 0.05 in molar basis. The three MED columns have 20 stages each, while T-4 has 45 stages and a reflux ratio of 4.6. In the MED, the split fractions and reflux ratios were adjusted so as to match the condenser duty of T-1 with the reboiler duty of T-2, and the condenser duty of T-2 with the reboiler duty of T-3. In order to spare CW and reduce heat demand in T-4, tower T-3 has a partial condenser with vapor distillate only, while T-1 and T-2 produce saturated liquid distillates. The three distillates are mixed and fed to T-4. Any ethanol dragged with CO_2 in the vapor streams from the partial condensers in T-1, T-2 and T-4 is recovered and recycled after cooling of vapors to 35 °C.

Pinch Analysis was done inside Hierarchy block A400 in order to design an effective heat exchanger network (E-1 to E-9 in Fig. A-5, Supp. Material) capable of recovering heat from hot streams and minimizing utility usage to pre-heat feed streams. Distillation bottoms consist mainly of water with small amounts (<1 wt%) of acetic acid, which are recycled to the bioreactor. RadFrac model was used for all columns, with VLE modeling via method NRTL-HOC.

2.1.5. Power Generation Unit (A500)

A500 (Fig. A-6, Supp. Material) was designed as a combined Brayton/Rankine cycle due to the high efficiency associated with this cycle, reaching up to 60% (Bass et al., 2011). The gas turbine fuel is the off-gas from the bioreactor containing unconverted CO and H_2. CO_2 produced in fermentation reactions is also present at high concentration, but its separation would be too costly and therefore it is not considered here. Although the presence of CO_2 in the gas fuel will decrease its heating value, hence the power output, it has been reported that the dilution of syngas with nonflammable gases such as N_2 and CO_2 does not affect significantly the combustion efficiency, the temperature at the nozzle, or the combustion stability (Lee et al., 2012). On the other hand, adding diluents is an effective way of controlling and adjusting NOx emissions, due to the observed logarithmic relation between diluent heat capacity (mass flow rate multiplied by constant pressure heat capacity) and NOx reduction per unit power (Lee et al., 2012). The simulation of the gas turbine was based on the SGT-300 gas turbine by Siemens (Siemens, 2009). A pressure ratio of 14 was set in the stage of air compression (C-2) and a slightly higher ratio, *i.e.* 14.2, was used in the compression of fuel gas(C-1). The air flow rate was set so that the exhaust gas would achieve a temperature of 545 °C at the turbine outlet, implying a temperature at the expander inlet, after combustion, of around 1050 °C. This is in agreement with other reports of gas turbine temperature profiles (*e.g.* Wärtsilä (2016) reports temperatures between 1200 °C and 1400 °C at the expander inlet). The hot flue gas from the gas turbine is split in two streams: *(i)* H-GAS-3 is sent to A200 for steam generation; and *(ii)* FG-E1 is sent to the boiler E-1 in the Rankine Cycle. All machines – compressors, gas turbine, steam turbine and pump – operate with adiabatic efficiency of 85%. The total output power generated in A500 is represented by the dotted line stream EE-T.

2.2. Financial analysis

The simulation results were used to create a financial model capable of predicting the Net Present Value (*NPV*) according to ethanol selling price. The model was then used to estimate the minimum ethanol selling price (*MESP*) for the production profile obtained in the designed process, that is, the ethanol selling price for *NPV* break-even ($NPV = 0$), assuming an Internal Rate of Return $IRR = 10\%$ (Aden et al., 2002).

The platform used for model construction was the MS Excel program CAPCOST, conceived and made available by Turton et al. (2008). CAPCOST estimates capital cost through a module costing technique and uses programmed functions to perform Cash Flow Analysis and Monte Carlo simulations. In this study the investment assumptions are based on the grassroots cost, *i.e.* the cost of building a completely new plant on a new land. Main assumptions for the financial analysis are summarized in Table 2. The base year is 2015, therefore the prices were adjusted to a CEPCI (Chemical Engineering Plant Cost Index) of 542.8, as published for November

Table 2
Main assumptions for financial evaluation.

Project life	20 years
Construction period	2 years
Hours per operating year	8328
Taxation rate	35%
Annual interest rate	10%
Salvage value	0
Depreciation method	Straight line
Cost of land	US$1,250,000
Working capital (Turton et al., 2008)	$0.1(C_{RM} + FCI_L + C_{OL})$
Cost of operating labor	*10% OPEX*

C_{RM}: Cost of raw materials; FCI_L: fixed capital investment excluding land purchase. C_{OL}: cost of operating labor.

2015 (Chemical Engineering, 2016).

CAPEX, or the total capital investment, is obtained by summing up the grassroots cost, the land cost and the working capital. *OPEX* includes: *(i)* direct (variable) production costs (*DPC*), such as raw materials, labor and maintenance; *(ii)* fixed production costs (*FPC*), such as property taxes and insurance; and *(iii)* general expenses (*GE*), such as R&D and distribution. The assumptions considered for *OPEX* calculation were based on the common ranges reported by Peters and Timmerhaus (1991) and are presented in Table B-1 (Appendix B, Supp. Material).

2.2.1. Purchase cost of equipment (PCE) estimation

CAPCOST has a set of built-in equations to estimate *PCE* inside given ranges of operation (Turton et al., 2008). When operational capacity is found to be outside the allowed range for equations, one can consider extrapolation by the six-tenths-factor rule in Eq. (3) (Peters and Timmerhaus, 1991). *PCE* for the following types of equipment were calculated directly on CAPCOST: compressors, steam turbine, electric drives, heat exchangers, blowers, pumps (with drives), distillation and absorption towers, fermenters, and gas turbine. Sizes (or capacities) for the equipment were obtained from results of material and energy balances calculated in Aspen.

To estimate the capital cost of the bioreactors, the vessels were assumed to have 975 m^3, with 80% of working capacity and operation under atmospheric pressure at the top of the vessel. The total volume of fermentation, calculated as explained in Sec. 2.1.3, was then used to find the required number of vessels. It is worth mentioning that, although fermentation stirred-tanks in the industry today have between 100 and 500 m^3 of capacity, the maximum practical volume is expected to be in the range of 800–1500 m^3 (Moulijn et al., 2013). According to Humbird and Fei (2016), who simulated the oxygen transfer rate for different liquid volumes, increasing the vessel size up to 1000 m^3 would not affect significantly the cost of gas supply, as the power required for a given gas transfer rate would increase approximately linearly with the liquid volume. However, the authors do point out a practical and economic limit of 1000 m^3 per vessel.

For equipment costs that were not available in the CAPCOST database, other references were consulted and prices were adjusted to proper year and capacity. For such cases, the sources and results are detailed in Tables B-4 (gasification unit), B-5 (microfiltration) and B-6 (cooling tower) of the Supp. Material. Assumptions considered for the water chiller are also listed in the Supp. Material (Table B-3).

$$cost\ at\ capacity\ A = \ cost\ at\ capacity\ B \times \left(\frac{capacity\ A}{capacity\ B}\right)^{0.6} \quad (3)$$

2.2.2. Costs of raw materials (C_{RM}), wastewater treatment (C_{WT}) and utilities (C_{UT})

Sugarcane bagasse is the most relevant raw material, accounting for nearly 90% of total C_{RM}. For the base evaluation, it is assumed that its delivered cost is 38 US$ per dry metric ton (Jacques, 2016). Other raw materials costs were retrieved from elsewhere and adjusted to the year 2015 (see Table B-7, Supp. Material): gasifier bed material (Dutta et al., 2011), tar reformer catalyst (Dutta et al., 2011), CW tower antifouling chemicals (Turton et al., 2008) and process water (Dutta et al., 2011). Wastewater treatment, required for liquid purges, is assumed to cost 0.06 US$/$m^3$ of wastewater based on the cost of tertiary treatment suggested in (Turton et al., 2008) updated to 2015 price. Waste disposal of gasifier ashes is assumed to cost 36 US$ per metric ton (Turton et al., 2008).

The utilities used in the process include: 2.5 bar steam, 10 bar steam, electricity, cooling water (30 °C–40 °C) and chilled water (15 °C–25 °C). All utilities are produced inside the plant, *i.e.* $C_{UT} = 0$, and the consumption rates (including electricity from pumps and compressors, cooling water, and heating) were calculated directly in Aspen simulations, excepting the fermenter stirring, which was assumed to demand 0.45 kW per cubic meter of liquid (Heinzle et al., 2006).

2.2.3. Monte Carlo simulation (MCS)

After building the base financial model, Monte Carlo simulations were performed to account for uncertainties in the economic evaluation. MCS works by repeatedly calculating an objective function after randomly sampling input parameter values out of specified probability distributions. In this study, the Net Present Value (*NPV*) was selected as the objective function and the uncertain input parameters were chosen to be the fixed capital investment FCI_L (excluding land purchase cost) and the cost of raw materials (C_{RM}). Since the factorial estimate of capital cost used in this study is usually associated with an accuracy of ±30% (Peters and Timmerhaus, 1991), FCI_L was put to vary within this range. The cost of raw materials, as defined in Sec. 2.2.2, was chosen to vary within a range of ±70%. MCS was specifically used to find the probability of obtaining non-negative *NPV*, assuming the aforementioned uncertainties, under different ethanol selling prices.

3. Results and discussion

3.1. Simulation

Design choices presented in Sec. 2.1 resulted in a production capacity of 71,000 m^3/year of E100, corresponding to approximately 0.33 m^3 per dry metric ton of feedstock. Table 3 presents a comparison with other studies regarding ethanol yield and LHV-based energy efficiency (η_{LHV}), *i.e.* the ratio between LHV in ethanol product and LHV in the dry feedstock. Given that the process was designed to achieve energy self-sufficiency, electricity production in the Combined Cycle (A500) was only slightly above the total requirement of the plant, reaching 1280 kWh/m^3, or 50 kWh/m^3 of electricity surplus.

Carbon conversion from biomass to ethanol was found to be just below 30%, a similar result to the one reported by Humbird et al. (2011) for the conceptual design of biochemical conversion of corn stover to ethanol. Although the feedstocks and other parameters are different, this result is an example refuting the common argument that thermochemical routes are inherently more carbon efficient due to full utilization of biomass components in the gasifier. Although carbon from biomass can be fully consumed in gasification, it is not necessarily all converted to syngas, as part of it might be sacrificed for energy generation in combustion reactions. While high carbon to syngas conversions of 95–99% can be achieved in directly-heated (partial-oxidation) fluidized gasifiers, indirectly-heated systems like the one considered here usually achieve lower conversions of 60–75%, in return of producing better quality syngas (Brown, 2011). Indeed, in the present study, only about 60% of carbon conversion to syngas was achieved, with the remaining carbon leaving as CO_2. Nonetheless, there is indisputable advantage in indirect heating systems in comparison with direct systems that would require air or pure oxygen. If air is used, then the syngas will be highly diluted with N_2, causing the fugacities of CO and H_2 in the gas phase to be lower and therefore seriously hindering the fermentation step due to the reduction of the mass transfer rates of these compounds. On the other hand, using O_2 would require the insertion of an Air Separation Unit (ASU), which is an expensive process in terms of energy and cost, both capital and operating types (Bhattacharya et al., 2012).

Table 3
Comparison of main results with other works.

	This study	Dutta et al., 2011	Porzio et al., 2012	Wei et al., 2009	Wei et al., 2009
Route	TB	TC	B (SSCF)	B (HF)	TB
Feedstock	Sugarcane bagasse	Pine chips	Poplar	Hardwood chips	Hardwood chips
Ethanol yield (m^3 per dry metric ton)	0.330	0.318	0.303–0.316	0.205	0.324
η_{LHV} (%)	38	40	35–37	24	37

TB: thermochemical-biochemical; TC: thermochemical-catalytic; B: biochemical; SSCF: simultaneous saccharification co-fermentation; HF: hydrolysis and fermentation.

Table 4 shows the syngas composition at the fermenter inlet, as well as the broth and the gas composition at the outlet. As explained in Sec. 2.1.1, a generic model of gasifier using the equilibrium approach under equilibrium-favoring conditions was preferred instead of adopting the results of a specific gasification plant. Nevertheless, the results herein presented are comparable to empirical results of steam gasification obtained elsewhere under similar temperature conditions: for example, Nipattummakul et al. (2011) reported the following syngas approximate (molar) composition for steam gasification of oil palm empty fruit branches between 900 °C and 1000 °C: 50% H_2, 25–30% CO, 14–19% CO_2. Moreover, the results are similar to those presented by NREL (Dutta et al., 2011) via simulation: 40.3% H_2, 9.4% CO_2, 32.3% CO, 16.2% H_2O, 1.5% CH_4.

The syngas composition calculated in the present study also contains small amounts of contaminants: 2 ppm NH_3, 196 ppm H_2S, 91 ppm HCl, 5 ppm COS. However, the model does not take into account the influence of these compounds on process variables such as pH and osmolarity or on the metabolism of the microorganisms. It is assumed that such levels of impurities are not enough to affect fermentation performance, damage the equipment or significantly alter the process in general. Although there is still a need for further research regarding tolerance limits to contaminants, there is evidence that syngas impurities such as HCN could achieve levels at which the process is potentially burdened (Lane, 2014). Other contaminants, such as H_2S and COS, were found insignificant unless at much higher concentrations (Vega et al., 1990).

Syngas fermentation does not require a specific H_2/CO ratio or the absence of CO_2 (Spath and Dayton, 2003), therefore the gas is assumed to be fed to the fermenter without any prior step of water-gas shift or CO_2 abatement for adjustment of composition. Yet, it is clear from Eqs. (1)–(2) that the gas composition is an important project parameter as it affects the availability of carbon (provided by CO or CO_2) and electrons (provided by H_2 or CO) for the microbial metabolism. For example, in the absence of H_2, the theoretical (*i.e.*maximum) carbon yield to ethanol (Y_{th}) will be 1/3, with the remaining carbon being oxidized to CO_2, according to Eq. (4) (Phillips et al., 1994). In the presence of H_2 and with H_2:CO $\leq$ 2, Y_{th} is predicted from Eq. (5), which is easily deduced from Eqs. (1)–(2). Furthermore, the presence of CO_2 in the substrate has been reported to increase product formation, although CO is consumed preferably (Heiskanen et al., 2007). In this case, it can be shown from Eqs. (1)–(2) that Y_{th} is calculated from Eq. (6). In all cases, it is evident from the equations that higher yields are obtainable when H_2 is provided with the gas. For the present design, the syngas composition presented in Table 4 would lead to a theoretical carbon yield of 0.68, while the actual carbon yield was obtained as 0.48. For comparison, other authors have reported carbon yields for different syngas molar compositions, such as: 0.24 for substrate containing 20% CO, 5% H_2, 15% CO_2 and 60% N_2 (Shen et al., 2014a); 0.28 for substrate containing 60% CO, 35% H_2 and 5% CO_2 (Richter et al., 2013).

Table 4
Composition of Syngas Substrate, Fermenter Off-Gas and Broth Outlet (wet basis).

	Syngas (mol %)	Off-gas (mol %)		Broth (wt%)
CO	26.3	6.4	C_2H_5OH	2.0
H_2	48.5	46.9	H_3CCOOH	0.5
CO_2	10.4	39.5	cells	0.3
H_2O	14.6	6.3	H_2O	97.2

$$CO + H_2O \xrightarrow{CODH} CO_2 + 2H^+ + 2e^- \quad (4)$$

where CODH ≡ carbon monoxide dehydrogenase.

$$Y_{th} = \frac{1}{3}\left(1 + \frac{x_{H_2}}{x_{CO}}\right) \quad [mol\ C/mol\ C] \quad (5)$$

$$Y_{th} = \frac{x_{CO} + x_{H_2}}{3\left(x_{CO} + x_{CO_2}\right)} \quad [mol\ C/mol\ C] \quad (6)$$

With concern to broth composition, simulation results are consistent with the experimental values reported in the reference used here as base for modeling, *i.e.* 23 g/L ethanol, 6 g/L acetate, 3 g/L cells (Gaddy et al., 2007), which is a good indication that the present model has performed well. The total volume required for fermentation would imply the use of nine fermentation vessels of 975 m^3 for the assumptions considered in this study.

Regarding water consumption, the process would require a freshwater usage of 11.6 m^3/m^3 E100, of which 82% are due to blowdown, windage and evaporative losses in the CW tower. An estimated range of 1.9–6 m^3/m^3 has been reported for lignocellulosic ethanol production (Aden, 2007). Since the present design considers water to be the main carrier of cooling, a first attempt on process improvement would be to include air-cooled heat exchangers whenever possible, for example in the condenser of the distillation tower. This could significantly reduce freshwater consumption, as shown by Martín et al. (2011). One should keep in mind, however, that air-cooling efficiency would be fairly compromised in tropical climate regions such as Brazil.

Energy requirements in the distillation unit (A400) were found to be 8700 MJ/m^3 with the use of multiple-effect distillation as pre-concentration step. This is lower than the estimated 10,500 MJ/m^3 by Piccolo and Bezzo (2007) for a 2.4 wt% broth obtained via the thermochemical-biochemical route, and higher than the range of 4400–6400 MJ/m^3 estimated in the same reference for three types of fully-biochemical routes, where the ethanol concentration in the broth is also higher, expected to be around 5 wt% (Hamelinck et al., 2005).

The requirements for the distillation towers, *i.e.* heating (Q_r) and cooling (Q_c), are depicted in Fig. 3, as a temperature-enthalpy flow diagram. The shaded areas indicate the distillation towers, of which T-1, T-2 and T-3 are heat integrated in the multiple-effect stack, and T-4 delivers the hydrous ethanol product. Fig. 3 evidences the reduction of external heat requirements accomplished with the MED system, which is effectively close to 1/3 of the total reboiler duty of the three pre-concentration columns. Vertical dotted lines indicate clearly the perfect matching of the reboiler with condenser

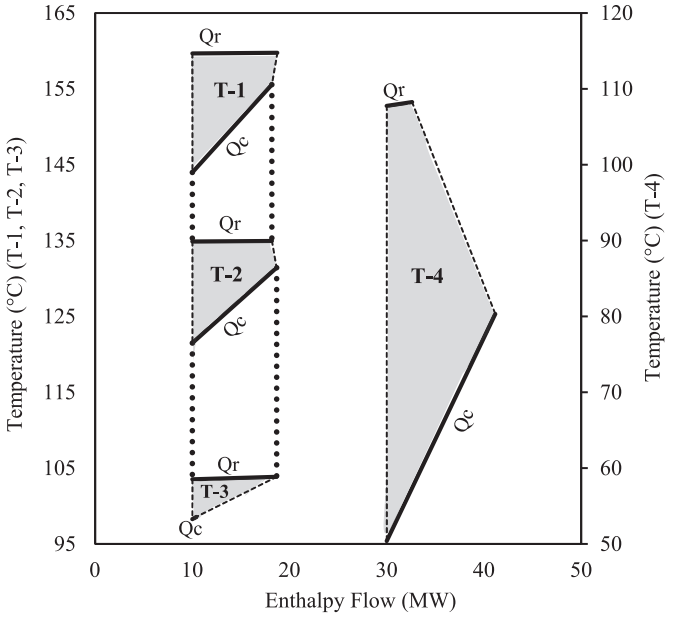

Fig. 3. Temperature enthalpy diagram for the distillation columns. The x-axis represents enthalpy flow changes.

duties between T-1 (6 bar) and T-2 (3 bar), and between T-2 and T-3 (1 bar). Fig. 3 also suggests the possibility of improving heat integration in the pre-concentration step by including in the MED stack a fourth column that could be positioned between T-2 and T-3, reducing the pre-concentration heat load by roughly 25%. It is also observable that T-4 has a low energy requirement, which is to some extent due to the fact that one of the feed streams, the distillate from T-3, is provided in the vapor phase. On the other hand, T-4 has a high requirement of CW due to the same reason.

3.2. Financial analysis

Table 5 summarizes the main economic results of the base model. *CAPEX* or the total capital investment, is consistent with other estimates for 2nd generation plants when considering the annual capacity, as presented in Fig. 4. An equivalent annual cost associated with *CAPEX* is also presented in Table 5. The *OPEX* is an important fraction of the *MESP*, as it makes up about 59% of costs and accounts to roughly twice the costs related to *CAPEX* (*i.e.* the return on investment (*ROI*) and depreciation). The minimum net profit represents the *ROI* associated with the *MESP*.

The overall contributions to *MESP* are depicted in Fig. 5 and a comparison with other works is presented in Fig. 6. Sugarcane bagasse is responsible for about 16% of the *MESP*, which is relatively low when compared to the feedstock contributions presented in Fig. 6 for other studies (Kazi et al., 2010). However, it is worth noting that these results consider other feedstocks, namely woody

Table 5
Main Economic Results (2016).

Grassroots cost	US$111.5 million
Plant *CAPEX*	US$125.15 million (US$14.7 million per year)
Plant *OPEX* [a]	US$29.6 million per year (417 US$/m^3)
Minimum net profit	US$9.7 million per year (136 US$/m^3)
Minimum ethanol selling price	706 US$/m^3

[a] Includes: costs of raw materials and waste treatment; labor costs; maintenance and repair; operating supplies; laboratory charges; patents and royalties; property taxes and insurance; plant overheads; administration; distribution and selling; and R&D.

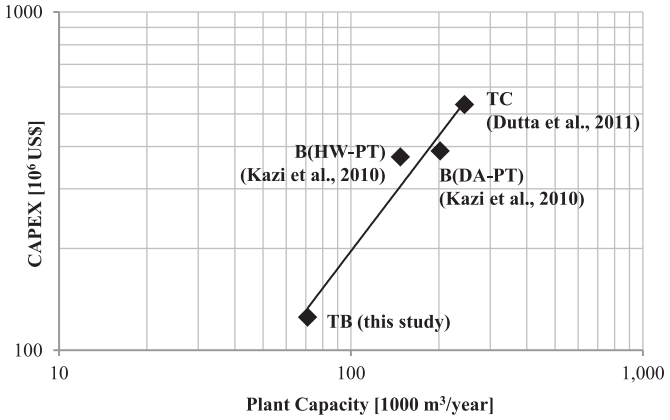

TB: thermochemical-biochemical; B: biochemical; HW-PT: hot water pretreatment; DA-PT: dilute acid pretreatment; TC: thermochemical-catalytic

Fig. 4. Comparison of *CAPEX* estimate with other studies. *CAPEX* results from other works were adjusted to 2015 prices.

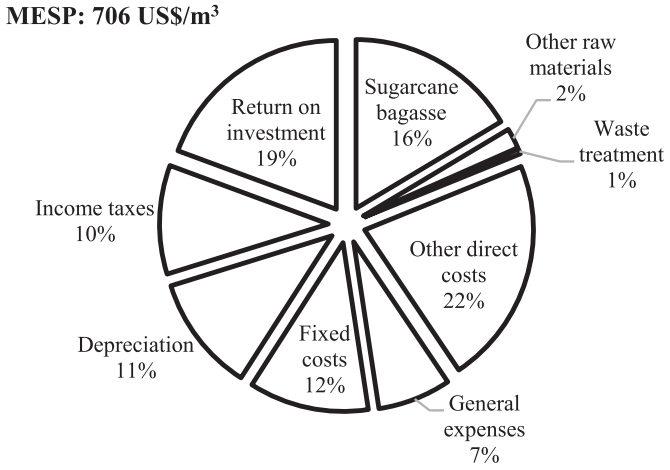

Fig. 5. Composition of *MESP*.

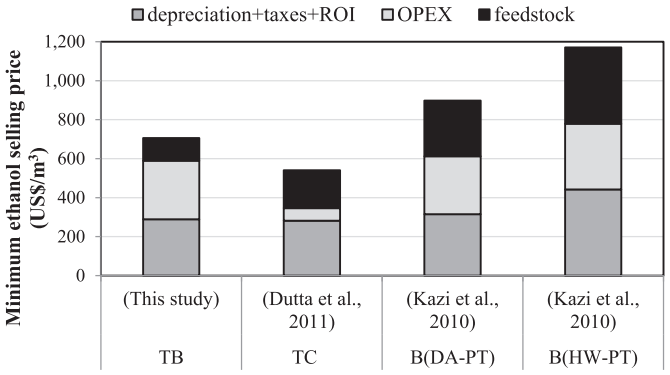

TB: thermochemical-biochemical; TC: thermochemical-catalytic; B: biochemical; DA-PT: dilute acid pre-treatment; HW-PT: hot water pre-treatment.

Fig. 6. Comparison of *MESP* composition with other studies. Feedstock cost is presented separately from other *OPEX* costs.

biomass and corn stover. Another report for 2nd-generation biochemical plants using sugarcane residues has shown that, similar to the present study, feedstock costs are estimated to make

up about 20% of costs (Jacques, 2016). Cheali et al. (2016) have shown that biomass conversion to ethanol through thermochemical-catalytic routes can indeed be advantageous over biochemical conversion depending on the characteristics of the feedstock (lignin and overall carbon content), despite the usually higher investments. For the assessment of four different scenarios varying the types of feedstock (poplar wood or corn stover) and conversion pathways (biochemical or thermochemical-catalytic), they found that feedstock costs contributed from 59 to 62.4%, with MESP ranging from \$500/m^3 to \$560/m^3, which is considerably lower than the result presented here. In a study on thermochemical-biochemical routes for bioethanol production from miscanthus, Roy et al. (2015) predicted ethanol production costs ranging from \$780/m^3 to \$900/m^3, however the results presented are not sufficient for further comparisons. An attractive picture was estimated by Martín and Grossmann (2011), with production costs ranging between \$0.84/gal (\$222/m^3) and \$1.07/gal (\$283/m^3), however, besides significant differences in their process flowsheet, their model makes several optimistic assumptions, particularly affecting separation costs, such as broth composition of 5 wt% of ethanol (or even 15 wt% in some scenarios), constant ethanol-water relative volatility of 2.2 and Fenske equation design in the distillation columns.

The current market price of E100, around \$450/m^3 (UNICA, 2016), is considerably lower than the predicted *MESP* in Table 5. Nevertheless, the results are comparable to predictions for other lignocellulosic ethanol processes, such as the ones presented in Fig. 6, and to the *MESP* estimated for existing biochemical-based plants: \$2.2/gal \$580/m^3) for Raizen, \$3.3/gal (\$870/m^3) for DuPont and \$4.6/gal (\$1220/m^3) for Abengoa (Jacques, 2016). Since those studies consider anhydrous ethanol, the results are expected to be slightly lower in the present study, which considers hydrous ethanol (dehydration by molecular sieves should contribute to operating costs with roughly \$0.05/kg (Cardona et al., 2010)).

Fig. 7 depicts the *NPV* cumulative probability curves obtained from MCS. The curves – from left to right – are relative to the values of the ethanol selling price for which the probability of achieving non-negative *NPV* is 20%, 40%, 60%, 80% and 100%. Non-negative *NPV* means the project has greater chances of being profitable than non-profitable. One could affirm, then, that the current process design would very likely attain profit for E100 selling prices above US\$780/m^3, even if the grassroots cost were found to be 30% higher than the base case and the raw materials

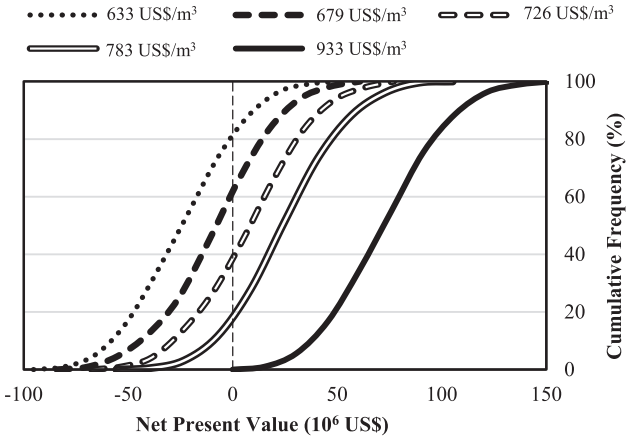

Fig. 7. *NPV* cumulative frequency distribution according to ethanol selling price. Curves show the probabilities of achieving non-negative *NPV*: 20% (dotted line); 40% (filled dashed line); 60% (unfilled dashed line); 80% (unfilled solid line); 100% (filled solid line).

were 70% more costly. At the other extreme, selling prices below US\$680/m^3 are less likely to provide positive results, but would still be feasible if optimistic conditions were to be achieved, with low values of feedstock price and capital investment.

4. Conclusions

This study presented a conceptual process design for the production of hydrous ethanol from sugarcane bagasse employing the so-called hybrid route based on gasification and syngas fermentation technology. The model is comprised of five distinct units that are integrated in a self-sufficient process in terms of energy (heat and power) and environment. Several steps of the process model are simplified due to a lack of reliable empirical data, for example, the model does not describe the effects of syngas contaminants on fermentation performance. In the same context, it is noteworthy that results of conversion, titer and yields in fermentation could vary significantly as observed with the high level of discrepancy among results reported in the literature. Hence, financial results could be substantially different if fermentation conditions diverged from the considerations made in this study. Nevertheless, the presented model has demonstrated to be a useful resource for the evaluation of technological potential of this route in comparison with other second generation technologies.

Simulation results indicate the potential to achieve energy self-sufficiency with an ethanol yield of 0.33 m^3 per metric ton of dry sugarcane bagasse, considering a production plant with annual capacity of 71,000 m^3. The financial analysis predicted the base case *MESP* to be 706 US\$/m^3. When considering uncertainties in the fixed capital investment and in the total cost of raw materials, the *MESP* ranges from 633 US\$/m^3 to 933 US\$/m^3, from low (20%) to high (100%) probability of achieving non-negative *NPV*. Even though the predicted ethanol selling prices are higher than the current market price of hydrous ethanol, the results demonstrate comparative potential for competitiveness in relation to other lignocellulosic ethanol technologies. Nonetheless, additional research is needed at different stages of the process to better understand and improve the technology, especially with regard to optimal conditions and reactor design for syngas fermentation, syngas cleaning requirements and efficient energy integration.

Acknowledgements

The authors acknowledge CAPES-BRAZIL, CTBE/CNPEM (Brazilian Bioethanol Science and Technology Laboratory), DSM and BE-Basic Foundation for financial support. This work is carried out as part of a Dual Degree PhD project under the agreement between UNICAMP and TU-DELFT.

Appendix A. Supplementary data

Supplementary data related to this article can be found at http://dx.doi.org/10.1016/j.jclepro.2017.01.165.

References

Aden, A., Ruth, M., Ibsen, K., Jechura, J., Neeves, K., Sheehan, J., Wallace, B., Montague, L., Slayton, A., Lukas, J., 2002. Lignocellulosic Biomass to Ethanol Process Design and Economics Utilizing Co-current Dilute Acid Prehydrolysis and Enzymatic Hydrolysis for Corn Stover, Report NREL/TP-510–32438. National Renewable Energy Laboratory (NREL), Golden, Colorado.

Aden, A., 2007. Water usage for current and future ethanol production. Southwest Hydrol. 6, 22–23.

Aspen Technology, 2011. Aspen Plus - Getting Started Modeling Processes with Solids.

Baratieri, M., Baggio, P., Fiori, L., Grigiante, M., 2008. Biomass as an energy source: thermodynamic constraints on the performance of the conversion process.

Bioresour. Technol. 99, 7063–7073. http://dx.doi.org/10.1016/j.biortech.2008.01.006.
Bass, R.J., Malalasekera, W., Willmot, P., Versteeg, H.K., 2011. The impact of variable demand upon the performance of a combined cycle gas turbine (CCGT) power plant. Energy 36, 1956–1965. http://dx.doi.org/10.1016/j.energy.2010.09.020.
Bhattacharya, A., Bhattacharya, A., Datta, A., 2012. Modeling of hydrogen production process from biomass using oxygen blown gasification. Int. J. Hydrogen Energy 37, 18782–18790. http://dx.doi.org/10.1016/j.ijhydene.2012.09.131.
Bonomi, A., Pinto, A., Charles, M., Farias De Jesus, D., Coutinho, H., Franco, J., Cunha, M.P., Oliveira De, M., Dias, S., Ferreira, M., Otávio, C., Paulo, C., Mantelatto, E., Maciel, R., Tassia, F., Junqueira, L., 2011. Technological Assessment Program (PAT) - the Virtual Sugarcane Biorefinery (VSB). Report. Brazilian Bioethanol Science and Technology Laboratory (CTBE), Brazilian Center for Research in Energy and Materials (CNPEM), São Paulo, Brazil.
Brown, R.C., 2011. Thermochemical Processing of Biomass: Conversion into Fuels, Chemicals and Power, Thermochemical Processing of Biomass: Conversion into Fuels, Chemicals and Power. http://dx.doi.org/10.1002/9781119990840.
Cardona, C.A., Sanchez, O.J., Gutierrez, L.F., 2010. Process Synthesis for Fuel Ethanol Production. CRC Press, Florida, USA.
Cheali, P., Posada, J.A., Gernaey, K.V., Sin, G., 2015. Upgrading of lignocellulosic biorefinery to value-added chemicals: sustainability and economics of bio-ethanol-derivatives. Biomass Bioenergy 75, 282–300. http://dx.doi.org/10.1016/j.biombioe.2015.02.030.
Cheali, P., Posada, J.A., Gernaey, K.V., Sin, G., 2016. Economic risk analysis and critical comparison of optimal biorefinery concepts. Biofuels Bioprod. Bioref. 10, 435–445. http://dx.doi.org/10.1002/bbb.1654.
Chemical Engineering Magazine, 2016. Issue of March 2016.
Chiang, T.-P., Luyben, W.L., 1983. Comparison of energy consumption in five heat-integrated distillation configurations. Ind. Eng. Chem. Process Des. Dev. 22, 175–179.
Choi, D.W., Chipman, D.C., Bents, S.C., Brown, R.C., 2010. A techno-economic analysis of polyhydroxyalkanoate and hydrogen production from syngas fermentation of gasified biomass. Appl. Biochem. Biotechnol. 160, 1032–1046. http://dx.doi.org/10.1007/s12010-009-8560-9.
Dias, M.O.S., Modesto, M., Ensinas, A.V., Nebra, S.A., Filho, R.M., Rossell, C.E.V., 2011. Improving bioethanol production from sugarcane: evaluation of distillation, thermal integration and cogeneration systems. Energy 36, 3691–3703. http://dx.doi.org/10.1016/j.energy.2010.09.024.
Dutta, A., Talmadge, M., Hensley, J., Worley, M., Dudgeon, D., Barton, D., Groenendijk, P., Ferrari, D., Stears, B., Searcy, E.M., Wright, C.T., Hess, J.R., 2011. Process Design and Economics for Conversion of Lignocellulosic Biomass to Ethanol. Report NREL/TP-5100–51400. National Renewable Energy Laboratory (NREL), Golden, Colorado.
Esmaili, E., Mostafavi, E., Mahinpey, N., 2016. Economic assessment of integrated coal gasification combined cycle with sorbent CO2 capture. Appl. Energy 169, 341–352. http://dx.doi.org/10.1016/j.apenergy.2016.02.035.
Fernández-Dacosta, C., Posada, J.A., Kleerebezem, R., Cuellar, M.C., Ramirez, A., 2015. Microbial community-based polyhydroxyalkanoates (PHAs) production from wastewater: techno-economic analysis and ex-ante environmental assessment. Bioresour. Technol. 185, 368–377. http://dx.doi.org/10.1016/j.biortech.2015.03.025.
Gaddy, J.L., Arora, D.K., Ko, C.-W., Phillips, J.R., Basu, R., Wikstrom, C.V., Clausen, E.C., 2007. Methods for Increasing the Production of Ethanol from Microbial Fermentation. US 7,285,402 B2.
Hamelinck, C.N., Van Hooijdonk, G., Faaij, A.P.C., 2005. Ethanol from lignocellulosic biomass: techno-economic performance in short-, middle- and long-term. Biomass Bioenergy 28, 384–410. http://dx.doi.org/10.1016/j.biombioe.2004.09.002.
Heiskanen, H., Virkajärvi, I., Viikari, L., 2007. The effect of syngas composition on the growth and product formation of Butyribacterium methylotrophicum. Enzyme Microb. Technol. 41, 362–367. http://dx.doi.org/10.1016/j.enzmictec.2007.03.004.
Heinzle, E., Biwer, A.P., Cooney, C.L., 2006. Development of Sustainable Bioprocesses. John Wiley & Sons, Ltd, Chichester, UK. http://dx.doi.org/10.1002/9780470058916.
Henley, E.J., Seader, J.D., 1981. Equilibrium-stage Separation Operations in Chemical Engineering. Johh Wiley & Sons, Inc., New York.
Humbird, D., Davis, R., Tao, L., Kinchin, C., Hsu, D., Aden, A., Schoen, P., Lukas, J., Olthof, B., Worley, M., Sexton, D., Dudgeon, D., 2011. Process Design and Economics for Biochemical Conversion of Lignocellulosic Biomass to Ethanol – Dilute-acid Pretreatment and Enzymatic Hydrolysis of Corn Stover. Report NREL/TP-5100–47764. National Renewable Energy Laboratory (NREL), Golden, Colorado.
Humbird, D., Fei, Q., 2016. Scale-up Considerations for Biofuels, in: Biotechnology for Biofuel Production and Optimization, pp. 513–537. http://dx.doi.org/10.1016/B978-0-444-63475-7.00020-0.
Jacques, C., 2016. News and Events – Raizen Has Lowest Price as Cellulosic Ethanol Hinges on Feedstock Cost. http://www.luxresearchinc.com/news-and-events/press-releases/read/raizen-has-lowest-price-cellulosic-ethanol-hinges-feedstock-cost. Accessed 08.03.2016.
Kazi, F.K., Fortman, J., Anex, R., Kothandaraman, G., Hsu, D., Aden, A., Dutta, A., 2010. Techno-economic Analysis of Biochemical Scenarios for Production of Cellulosic Ethanol. Report NREL/TP-6A2–46588. National Renewable Energy Laboratory (NREL), Golden, Colorado.
Klasson, K.T., Ackerson, M.D., Clausen, E.C., Gaddy, J.L., 1991. Bioreactor design for synthesis fermentations. Fuel 70, 605–614.
Klasson, K.T., Ackerson, C.M.D., Clausen, E.C., Gaddy, J.L., 1992. Biological conversion of synthesis gas into fuels. Int. J. Hydrogen Energy 17, 281–288. http://dx.doi.org/10.1016/0360-3199(92)90003-F.
Lane, J., 2015. Steel's Big Dog Jumps into Low Carbon Fuels: ArcelorMittal, LanzaTech, Primetals Technologies to Construct $96M Biofuel Production Facility. Biofuels Dig. http://www.biofuelsdigest.com/bdigest/2015/07/13/steels-big-dog-jumps-into-low-carbon-fuels-arcelormittal-lanzatech-primetals-technologies-to-construct-96m-biofuel-production-facility/. Accessed 08.03.2016.
Lane, J., 2014. On the Mend: Why INEOS Bio Isn't Producing Ethanol in Florida. Biofuels Dig. http://www.biofuelsdigest.com/bdigest/2014/09/05/on-the-mend-why-ineos-bio-isnt-reporting-much-ethanol-production/. Accessed 08.03.2016.
Lee, M.C., Seo, S. Bin, Yoon, J., Kim, M., Yoon, Y., 2012. Experimental study on the effect of N_2, CO_2, and steam dilution on the combustion performance of H_2 and CO synthetic gas in an industrial gas turbine. Fuel 102, 431–438. http://dx.doi.org/10.1016/j.fuel.2012.05.028.
Linnhoff, B., Dunford, H., Smith, R., 1983. Heat integration of distillation columns into overall processes. Chem. Eng. Sci. 38, 1175–1188.
Martín, M., Ahmetovic, E., Grossmann, I.E., 2011. Optimization of water consumption in second generation bioethanol plants. Ind. Eng. Chem. Res. 50, 3705–3721. http://dx.doi.org/10.1021/ie101175p.
Martín, M., Grossmann, I.E., 2011. Energy optimization of bioethanol production via gasification of switchgrass. AIChE J. 57, 3408–3428. http://dx.doi.org/10.1002/aic.12544.
Moulijn, J.A., Makkee, M., van Diepen, A.E., 2013. Chemical Process Technology. Wiley, Chichester, UK.
Nipattummakul, N., Ahmed, I.I., Gupta, A.K., Kerdsuwan, S., 2011. Hydrogen and syngas yield from residual branches of oil palm tree using steam gasification. Int. J. Hydrogen Energy 36, 3835–3843. http://dx.doi.org/10.1016/j.ijhydene.2010.04.102.
Palacios-Bereche, R., Ensinas, A.V., Modesto, M., Nebra, S.A., 2015. Double-effect distillation and thermal integration applied to the ethanol production process. Energy 82, 512–523. http://dx.doi.org/10.1016/j.energy.2015.01.062.
Parikh, J., Channiwala, S.A., Ghosal, G.K., 2005. A correlation for calculating HHV from proximate analysis of solid fuels. Fuel 84, 487–494. http://dx.doi.org/10.1016/j.fuel.2004.10.010.
Peters, M.S., Timmerhaus, K.D., 1991. Plant Design and Economics for Chemical Engineers. McGraw-Hill, New York.
Phillips, J.R., Clausen, E.C., Gaddy, J.L., 1994. Synthesis gas as substrate for the biological production of fuels and chemicals. Appl. Biochem. Biotechnol. 45–46, 145–157. http://dx.doi.org/10.1007/BF02941794.
Piccolo, C., Bezzo, F., 2007. Ethanol from lignocellulosic biomass: a comparison between conversion technologies. Comput. Aided Chem. Eng. 24, 1277–1282. http://dx.doi.org/10.1016/S1570-7946(07)80237-9.
Piccolo, C., Bezzo, F., 2009. A techno-economic comparison between two technologies for bioethanol production from lignocellulose. Biomass Bioenergy 33, 478–491. http://dx.doi.org/10.1016/j.biombioe.2008.08.008.
Porzio, G.F., Prussi, M., Chiaramonti, D., Pari, L., 2012. Modelling lignocellulosic bioethanol from poplar: estimation of the level of process integration, yield and potential for co-products. J. Clean. Prod. 34, 66–75. http://dx.doi.org/10.1016/j.jclepro.2012.01.028.
Puig-Arnavat, M., Bruno, J.C., Coronas, A., 2010. Review and analysis of biomass gasification models. Renew. Sustain. Energy Rev. 14, 2841–2851. http://dx.doi.org/10.1016/j.rser.2010.07.030.
Rajagopalan, S., Datar, R.P., Lewis, R.S., 2002. Formation of ethanol from carbon monoxide via a new microbial catalyst. Biomass Bioenergy 23, 487–493. http://dx.doi.org/10.1016/S0961-9534(02)00071-5.
Ramzan, N., Ashraf, A., Naveed, S., Malik, A., 2011. Simulation of hybrid biomass gasification using Aspen plus: a comparative performance analysis for food, municipal solid and poultry waste. Biomass Bioenergy 35, 3962–3969. http://dx.doi.org/10.1016/j.biombioe.2011.06.005.
Richter, H., Martin, M.E., Angenent, L.T., 2013. A two-stage continuous fermentation system for conversion of syngas into ethanol. Energies 6, 3987–4000. http://dx.doi.org/10.3390/en6083987.
Roy, P., Dutta, A., Deen, B., 2015. Greenhouse gas emissions and production cost of ethanol produced from biosyngas fermentation process. Bioresour. Technol. 192, 185–191. http://dx.doi.org/10.1016/j.biortech.2015.05.056.
Shen, Y., Brown, R., Wen, Z., 2014a. Syngas fermentation of Clostridium carboxidivoran P7 in a hollow fiber membrane biofilm reactor: evaluating the mass transfer coefficient and ethanol production performance. Biochem. Eng. J. 85, 21–29. http://dx.doi.org/10.1016/j.bej.2014.01.010.
Shen, Y., Brown, R., Wen, Z., 2014b. Enhancing mass transfer and ethanol production in syngas fermentation of Clostridium carboxidivorans P7 through a monolithic biofilm reactor. Appl. Energy 136, 68–76. http://dx.doi.org/10.1016/j.apenergy.2014.08.117.
Shen, Y., Jarboe, L., Brown, R., Wen, Z., 2015. A thermochemical-biochemical hybrid processing of lignocellulosic biomass for producing fuels and chemicals. Biotechnol. Adv. 33, 1799–1813. http://dx.doi.org/10.1016/j.biotechadv.2015.10.006.
Siemens, A.G., 2009. SGT-300 Industrial Gas Turbine. Brochure. Siemens Energy, Inc. http://www.energy.siemens.com/hq/pool/hq/power-generation/gas-turbines/SGT-300/Brochure%20Gas%20Turbine%20SGT-300%20for%20Power%20Generation.pdf. Accessed 11.26.2016.

Silva, V.B., Rouboa, A., 2014. Predicting the syngas hydrogen composition by using a dual stage equilibrium model. Int. J. Hydrogen Energy 39, 331–338. http://dx.doi.org/10.1016/j.ijhydene.2013.10.053.

Souza, G.M., Victoria, R.L., Joly, C.A., Verdade, L.M., 2015. Bioenergy and Sustainability: Bridging the Gaps, SCOPE Briefing. http://dx.doi.org/10.1017/CBO9781107415324.004.

Spath, P.L., Dayton, D.C., 2003. Preliminary Screening – Technical and Economic Assessment of Synthesis Gas to Fuels and Chemicals with Emphasis on the Potential for Biomass-derived Syngas, NREL Technical Report NREL/TP-510–34929. National Renewable Energy Laboratory (NREL), Golden, Colorado.

Turton, R., Bailie, R.C., Whiting, W.B., Shaeiwitz, J.A., 2008. Analysis, Synthesis and Design of Chemical Processes, Prentice Hall International Series in the Physical and Chemical Engineering Sciences. Pearson Education, Michigan, USA.

UNICA, 2016. Sugarcane Industry Association. Report. http://www.unicadata.com.br. Accessed 06.13.2016.

Van der Heijden, H., Ptasinski, K.J., 2012. Exergy analysis of thermochemical ethanol production via biomass gasification and catalytic synthesis. Energy 46, 200–210. http://dx.doi.org/10.1016/j.energy.2012.08.036.

Vega, J.L., Klasson, K.T., Kimmel, D.E., Clausen, E.C., Gaddy, J.L., 1990. Sulphur gas tolerance and toxicity of CO-utilizing bacteria. Appl. Biochem. Biotechnol. 24/25, 329–340.

Vega, J.L., Prieto, S., Elmore, B.B., Clausen, E.C., Gaddy, J.L., 1989. The Biological production of ethanol from synthesis gas. Appl. Biochem. Biotechnol. 20–21, 781–797. http://dx.doi.org/10.1007/BF02936525.

Wagner, H., Kaltschmitt, M., 2012. Biochemical and thermochemical conversion of wood to ethanol—simulation and analysis of different processes. Biomass Convers. Biorefin. 3, 87–102. http://dx.doi.org/10.1007/s13399-012-0064-0.

Wankat, P.C., 1993. Multieffect distillation processes. Ind. Eng. Chem. Res. 32, 894–905. http://dx.doi.org/10.1021/ie00017a017.

Wärtsilä, 2016. Gas turbine for Power Generation: Introduction. http://www.wartsila.com/energy/learning-center/technical-comparisons/gas-turbine-for-power-generation-introduction. Accessed 12.01.2016.

Wei, L., Pordesimo, L.O., Igathinathane, C., Batchelor, W.D., 2009. Process engineering evaluation of ethanol production from wood through bioprocessing and chemical catalysis. Biomass Bioenergy 33, 255–266. http://dx.doi.org/10.1016/j.biombioe.2008.05.017.

Worley, M., Yale, J., 2012. Biomass Gasification Technology Assessment. Consolidated Report NREL/SR-5100–57085. National Renewable Energy Laboratory (NREL), Golden, Colorado.

Younesi, H., Najafpour, G., Mohamed, A.R., 2005. Ethanol and acetate production from synthesis gas via fermentation processes using anaerobic bacterium, Clostridium ljungdahlii. Biochem. Eng. J. 27 (2), 110–119. http://dx.doi.org/10.1016/j.bej.2005.08.015.